AD-A194 217 ANALYSIS OF FREE ELECTRON LASER PERFORMANCE UTILIZING 1/1
THE NATIONAL BUREAU (U) NATIONAL BUREAU OF STANDARDS
GAITHERSBURG MD C TANG ET AL. 1987 N00014-87-F-0066
UNCLASSIFIED F/G 20/7 NL

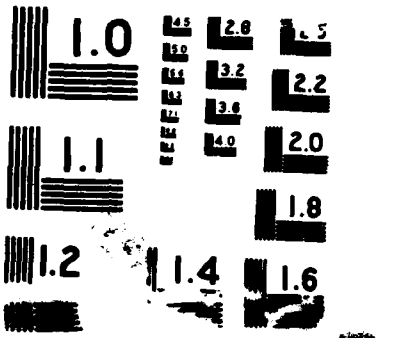
1.0
1.1
1.2
1.4
1.6
1.8
2.0
2.2
2.8
3.2
3.6
4.0

AD-A194 217

DTIC FILE COPY

DTIC SELECTE APR 25

ANALYSIS OF FREE ELECTRON LASER PERFORMANCE UTILIZING THE NATIONAL BUREAU OF STANDARDS' CW MICROTRON*

Cha-Mei Tang and Phillip Sprangle
Plasma Physics Division, Naval Research Laboratory, Washington, D.C. 20375-5000

Samuel Penner and Xavier K. Maruyama
Center for Radiation Research, National Bureau of Standards, Gaithersburg, MD 20899

Abstract

The National Bureau of Standards' (NBS) CW racetrack microtron (RTM) will be utilized as a driver for a free electron laser (FEL) oscillator. The NBS RTM possesses many exceptional properties of value for the FEL: i) CW operation, ii) energy from 20-185 MeV, iii) small energy spread and emittance, iv) excellent energy stability, and v) high average power. The 1-D FEL gain formula predicts that the FEL would oscillate at the fundamental approximately from 0.25 μm to 10 μm when up-grading the peak current to $\geq$ 2 A. In this paper, we present 3-D self-consistent numerical results including several realistic effects, such as emittance, betatron oscillations, diffraction and refraction. The results indicate that the design value of the transverse emittance is small enough that it does not degrade the FEL performance for intermediate to long wavelengths, and only slightly degrades the performance at the shortest wavelength under consideration. Due to the good emittance, the current density is high enough that focusing, or guiding, begins to manifest itself for wavelengths > 2.0 μm.

Introduction

An FEL facility for applications, primarily in biomedical and material science research as well as for basic physics and chemistry, is to be situated at the National Bureau of Standards[1,2]. A CW 185 MeV racetrack microtron (RTM)[3] is under construction. The NBS Accelerator Laboratory consists of a series of interconnected, individually shielded, underground halls. The updated layout is indicated in Figure 1. The FEL is expected to be operational by 1990.

The major limitation of an RTM as an FEL driver is that its peak current capability is lower than electron linacs which operate in the same energy range. However, the RTM is superior to pulsed linacs in energy spread and emittance. The RTM is comparable to a storage ring in terms of beam emittance and energy spread, but there is no restriction on insertion length or "stay clear" aperture. The beam energy can be varied continuously over a wide range without significant loss of performance. In addition, microtrons are compact and energy efficient. Because of the CW nature of the RTM, the generation of coherent photons is not hindered by a finite macropulse length.

* This work has been supported in part by the U.S. Office of Naval Research.

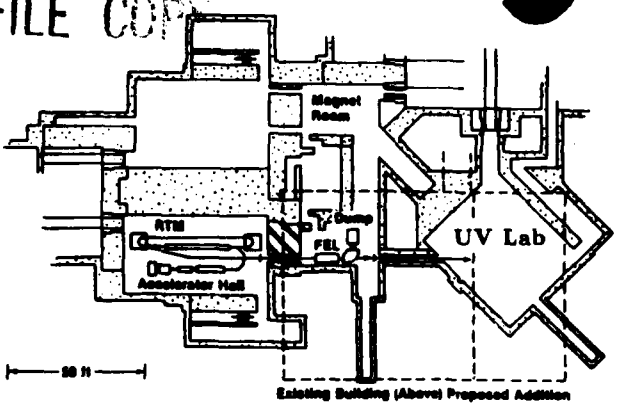

Fig. 1. Updated configuration for accelerator and FEL halls. The entire shielded complex is located 40 ft below ground level. Visible and infrared radiation will be directed to a ground level laboratory (indicated by the dashed lines) above the UV laboratory.

The original design parameters of the NBS RTM are given in Refs. 1-3. The design calculations indicate a longitudinal emittance $\epsilon_L < 30$ keV-degrees and a normalized transverse emittance[1,2] $\epsilon_N < 10$ mm-mrad. Based on recent measurements of the performance of the 5 MeV injector linac, the actual values of both the longitudinal and transverse emittance are expected to be smaller than the design values. The injector system must be upgraded to provide a peak current of ≥ 2 A in 3.5 psec micropulses, giving electron pulse length $\ell_{eb} \simeq 0.1$ cm. In order to keep the average electron beam power within the capability of the existing RF power system, the new injector will fill only a small fraction of the RF buckets (e.g., 1/24, 1/120 depending on electron beam energy). We are proceeding with a design of a photocathode injector system for this upgrade.

1-D Free Electron Laser Analysis

A first order evaluation of the FEL performance of the NBS RTM can be obtained from the 1-D small signal low gain formula[4]. The results indicate that sufficient gain can be obtained at fundamental wavelengths in the range from $10\ \mu m > \lambda > 0.25\ \mu m$. The formula for the electric field amplitude gain G in the small signal, low gain regime, can be written as

$$G = \frac{1}{2} F_1^2 \frac{\pi^2}{\sigma_R} \frac{I}{I_A} \frac{\lambda_w^2}{\gamma_o^3} K^2 N^3 \frac{\partial}{\partial \nu} \left(\frac{\sin \nu}{\nu} \right)^2 ,$$

This document has been approved for public release and sale; its distribution is unlimited.

U.S. Government work not protected by U.S. copyright.

88 4 22 053

where N is the number of wiggler periods, γ_o is the initial relativistic gamma factor, $\sigma_R = \pi r_o^2$ is the cross-sectional area of the radiation, r_o is the minimum $1/e$ radius of the Gaussian radiation field amplitude, $I_A = 17 \times 10^3$ A, I is the current in amperes, $K = (|e|B_w\lambda_w/2\pi m_o c^2)_{RMS}$ is the wiggler parameter, B_w is the magnetic field in the wiggler, λ_w is the wavelength of the wiggler, $F_1 = J_o(b) - J_1(b)$ for a linearly polarized wiggler, $b = K^2/2(1+K^2)$, $\nu = -N\lambda(\omega - \omega_s)/2c$ is the normalized frequency mismatch, and $\omega_o \sim 2\gamma^2 c(2\pi/\lambda_w)/(1 + K^2)$ is the resonant angular frequency. The function $\partial/\partial\nu(\sin\nu/\nu)^2$ has a maximum value of 0.54 when $\nu = -1.3$.

The power gain can be obtained by

$$G_p = (1 + G)^2 - 1.$$

In the low gain regime, $G_p \simeq 2G$. The FEL will oscillate when the power gain is greater than the losses per pass in the resonator.

The 1-D gain formula is only a rough estimate. It is sensitive to the choice of filling factor. We have chosen a filling factor which is smaller than the conventional by a factor of 2, so that the gain estimate is conservative.

The conceptual design consists of a linearly polarized wiggler with a period of $\lambda_w = 2.8$ cm, and a nominal magnetic field amplitude of $B_{wo} = 5400$ G. This can be constructed with a hybrid wiggler design with the gap separating the wiggler poles of $g = 1.0$ cm. A wiggler can be constructed conceptually in more than one section, such that a wiggler of shorter length can also be available. A shorter wiggler and a corresponding vacuum chamber may be necessary for long wavelength operation.

Figure 2 is a plot of the 1-D maximum small signal power gain versus wavelength, assuming a conservative peak current of 2 A. The open circles (o) are obtained with electron beam energies of 25, 50, 75, 125, and 175 MeV. The solid curves are obtained for the same electron beam energies, but varying the wiggler amplitude from $0.6B_{wo}$ to B_{wo}. The magnetic field in the wiggler is to be changed by varying the gap between the poles from 1.4 cm to 1.0 cm. As the magnetic field decreases, the wavelength of the radiation decreases, and the gain is reduced.

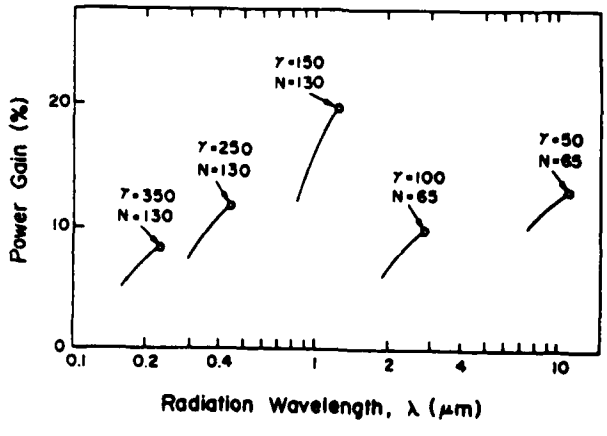

Fig. 2. Small signal power gain versus wavelength based on 1-D calculation.

3-D Effects on the Gain

Since FELs are not actually 1-D, 3-D effects will change the gain. Some of the 3-D effects that we will examine in this paper are finite transverse emittance, radiation diffraction and refraction, and some effects associated with finite-length electron pulses.

We will assess these three-dimensional effects using a fully 3-D self-consistent computer code, SHERA, developed at the Naval Research Laboratory. The formulation of the wave equation is based on the source dependent expansion[5-6] of the radiation field, and the electron dynamics[7] are evaluated self-consistently. We assume a waterbag distribution in the 4-D transverse emittance space, which leads to a parabolic profile for the electron beam density. Since the energy spread of the NBS RTM is very small, it will not be considered; and we will also not treat the effects of pulse slippage on the gain. The radiations are taken to have a Rayleigh length of 175 cm with the minimum radiation waist located at the center of the wiggler. Results for two different operating regimes will be presented.

The effect of the emittance on the performance of the FEL will be more important for short wavelength operations. Thus, our first example will be for $\lambda = 0.23$ μm with $\gamma_o = 350$. The pulse slippage distance, $N\lambda = 0.003$ cm, is much shorter than the electron pulse length, ℓ_{eb}. Plots of the power gain, G_p, versus the normalized frequency mismatch, ν, are shown in Figure 3. Curve (a) gives the 1-D estimate of the gain. Curves (b), (c) and (d) are the gains calculated from the computer code for normalized transverse emittance of ϵ_N =5, 10 and 20 mm mrad, respectively. The minimum $1/e$ radiation field amplitude waist is $r_o = 3.57 \times 10^{-2}$ cm. The matched edge radius of the electron beam is only a function of the normalized transverse emittance, independent of energy, assuming equal focusing in both transverse directions within the wiggler. The matched edge radii of the electron beam are $r_{eb} = 1.77 \times 10^{-2}$, 2.50×10^{-2} and 3.54×10^{-2} cm for normalized edge transverse emittances of ϵ_N = 5, 10 and 20 mm mrad, respectively. If the emittance becomes larger than 20 mm mrad, the radius of the electron beam will become larger than the radiation spot size, and the gain will be substantially reduced.

The effect of finite emittance on the gain is negligible for $\lambda = 1.25$ μm with $\gamma_o = 150$. The pulse slippage distance in this case is 0.016 cm, and it is still unimportant. Figure 4 shows plots of the power gain, G_p, versus the normalized frequency mismatch, ν, similar to Figure 3. Again, the curve (a) gives the 1-D estimate of gain. Curves (b), (c) and (d) are the gains calculated from the computer code for normalized emittance of ϵ_N =5, 10 and 20 mm mrad, respectively. Since the wavelength is longer, the minimum $1/e$ radiation field amplitude waist becomes $r_o = 8.3 \times 10^{-2}$ cm, and the electron beam radii are much smaller than the radiation waist. The gain at $\lambda = 1.25$ μm is virtually insensitive to the design value of the finite transverse emittance.

Figures 3 and 4 also show a shift of the zero crossing of the gain curves obtained from 3-D simulation. This shift comes from the change in the phase of the diffracting radiation field. It has no real important effect on the oscillation criteria for the examples under consideration.

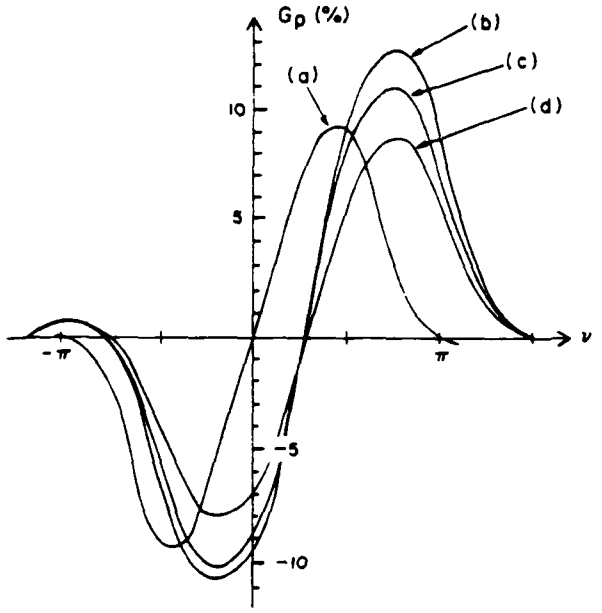

Fig. 3. Power gain, G_p, versus frequency mismatch, ν, at $\lambda = 0.23$ μm with $\gamma_o = 350$. Curve (a) is based on 1-D gain formula. Curves (b), (c) and (d) are obtained from simulations with normalized transverse edge emittances of $\epsilon_N = 5$, 10 and 20 mm mrad, respectively.

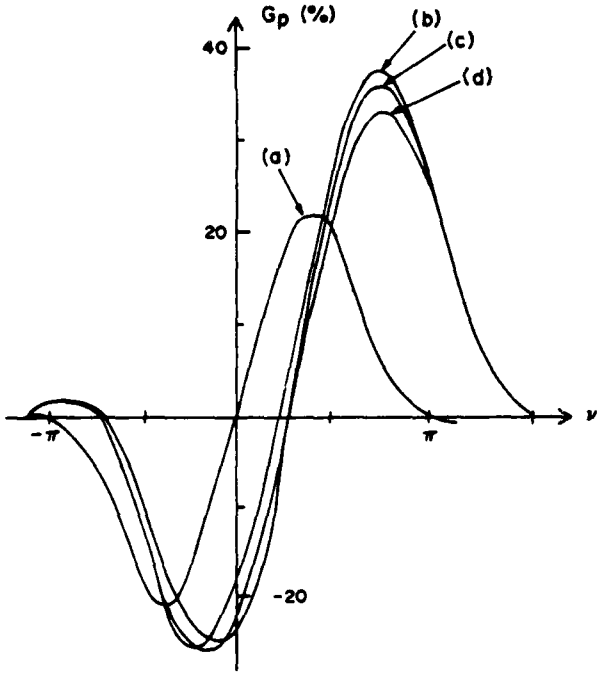

Fig. 4. Power gain, G_p, verus frequency mismatch, ν, at $\lambda = 1.25$ μm with $\gamma_o = 150$. Curve (a) is based on 1-D gain formula. Curves (b), (c) and (d) are obtained from simulations with normalized transverse edge emittances of $\epsilon_N = 5$, 10 and 20 mm mrad, respectively.

Since the current is a function of axial position in a finite length electron pulse, and pulse slippage is unimportant, the local gain is a function of the local current in the electron pulse. For the first example at $\lambda = 0.23$ μm with normalized transverse edge emittance $\epsilon_N = 10$ mm mrad, the simulations indicate that the gain is proportional to the local current, consistent with the 1-D formula. For the second example at $\lambda = 1.25$ μm, the gain increases faster than the linear power of the current. Figure 5 is a plot of normalized power gain, i.e., power gain from simulation divided by the maximum 1-D power gain, versus the frequency mismatch at $\lambda = 1.25$ μm with normalized transverse edge emittance $\epsilon_N = 10$ mm mrad for three different currents: (a) $I = 4.0$ A, (b) $I = 2.0$ A and (c) $I = 0.5$ A. We find that the normalized gain increases as current increases. This can be explained by the self-focusing or guiding phenomenon[5-6,8-11] of the FEL. This is most easily observed in the plots of the normalized $1/\epsilon$ Gaussian radiation field amplitude radius, shown in Figure 6. For $I = 0.5$ A, the radiation radius behaves like a free space resonator radiation field, curve (- - -). For $I = 2$ A, the radiation radius is less than the free space radius at the end of the wiggler as self-focusing begins to show, curve (——). If the current can be increased to 4 A, the radiation becomes even more focused, curve (.....). The reason that self-focusing is evident at such low current is that the emittance is very good and current density is high throughout the interaction region, i.e., high beam brightness $B_N = 2I/(\pi^2\epsilon_N^2) > 4 \times 10^9$ A/m^2/rad^2, where $I = 2$ A and edge emittance $\epsilon_N = 10$ mm mrad.

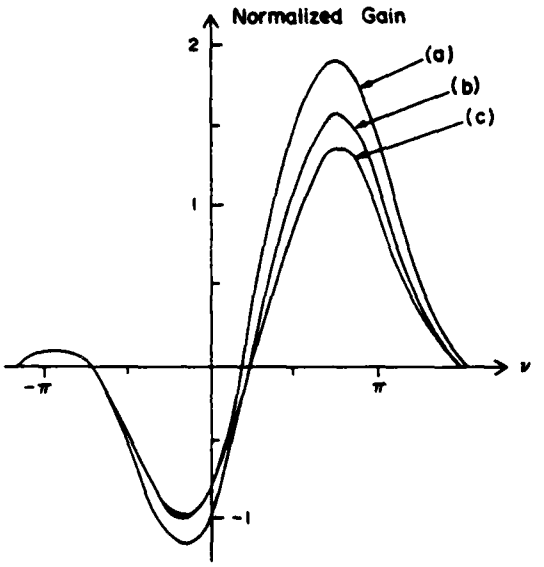

Fig. 5. Normalized gain versus frequency mismatch for $\lambda = 1.25$ μm and edge emittance of $\epsilon_N = 10$ mm mrad. Curves (a), (b) and (c) correspond to results obtained with currents of $I = 4.0$, 2.0, and 0.5 A, respectively.

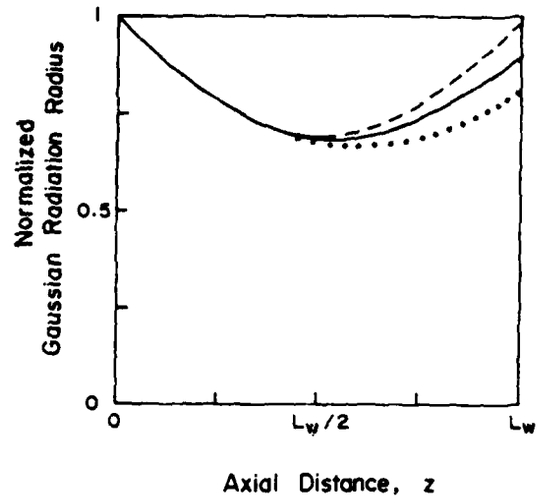

Fig. 6. Normalized $1/e$ Gaussian radiation field amplitude radius as a function of distance z in the wiggler with $\lambda = 1.25$ μm and edge emittance $\epsilon_N = 10$ mm mrad for three different currents: (- - -) $I = 0.5$ A, (——) $I = 2$ A and (.....) $I = 4$ A.

Conclusions

The 3-D self-consistent simulation results from the computer code SHERA indicate that the design value of the transverse emittance is very good, so that it does not degrade the FEL performance for intermediate to long wavelengths, and only slightly degrades the performance at the shortest wavelength under consideration compared to the gain obtained with even smaller emittance. Due to the good emittance, the current density is high enough that focusing, or guiding, begins to manifest itself for wavelengths > 2.0 μm.

References

[1] C.M. Tang, P. Sprangle, S. Penner, B.M. Kincaid and R.R. Freeman, Nucl. Instr. and Meth. A250, 278 (1986). Also in: Free Electron Lasers, Proc. 7th Int. Conf. on FELs, eds., E.T. Scharlemann and D. Prosnitz (North-Holland, Amsterdam, 1986) p. 278.

[2] X.K. Maruyama and S. Penner, C.M. Tang and P. Sprangle, to be published in the Proc. 8th Intl. Conf. on FELs.

[3] S. Penner et al., IEEE Trans. Nucl. Sci. NS-32, 2669 (1985).

[4] P. Sprangle, R.A. Smith and V.L. Granatstein, Infrared Millimeter Waves, Vol. I, ed., K.J. Button (Academic Press, New York, 1979) p. 279.

[5] P. Sprangle, A. Ting and C.M. Tang, accepted for publication in Phys. Rev. Lett. (1987) and P. Sprangle, A. Ting and C.M. Tang, accepted for publication in Phys. Rev. A (1987). Also submitted to the Proc. of the 8th Intl. FEL Conf., Glasgow, Scotland (1986).

[6] P. Sprangle, A. Ting, B. Hafizi and C. M. Tang, in this proceeding.

[7] C.M. Tang and P. Sprangle, IEEE J. of Quantum Elec QE-21, 970 (1985).

[8] P. Sprangle and C.M. Tang, Appl. Phys. Lett. 39, 67 (1981). Also in: C.M. Tang and P. Sprangle, Free-Electro Generator of Coherent Radiation, Physics of Quantum Electronics, Vol. 9, eds., S.F. Jacobs, G.T. Moore, H.S Pilloff, M. Sargent III, M.O. Scully, R. Spitzer (Eddison Wesley, Reading, MA, 1982) p. 627.

[9] E.T. Scharlemann, A.M. Sessler and J.S. Wurtele, Phys Rev. Lett. 54, 1925 (1985).

[10] G.T. Moore, Opt. Comm. 52, 46(11084), 54, 121 (1985).

[11] M. Xie and D.A.G. Deacon, same as ref. 1, p. 426.

Accession For
NTIS GRA&I
DTIC TAB
Unannounced
Justification per
By
Distribution/
Availability Codes
Dist | Avail and/or Special
A-1

QUALITY INSPECTED 4

END
DATED
FILM
8-88
DTIC